FLOW CONTROL OVER THE WING OF A FIGHTER-TYPE CONFIGURATION USING BOUNDARY LAYER SUCTION

M. R. Soltani, T. Khadivi, A. R. Davari
Department of Aerospace Engineering, Sharif University of Technology, Tehran, I. R. Iran

Keywords: *Cropped Delta Wing, Vortex, Flow Control, Suction, Sweep Angle*

Abstract

The objective of this study is to determine the effectiveness of using an active suction technique to delay flow separation over the wing of a fighter type configuration model. A number of experiments were conducted on a 40 degree swept cropped delta wing, similar to the High Alpha Research Vehicle (HARV) model, operating at two subsonic speeds and at low to moderate angles of attack. Both spanwise surface pressure distribution and velocity profiles at various angles of attack for suction on and off cases were measured. Smoke and tufts were used to visualize the flow over the wing at various angles of attack. The results indicate formation of a relatively weak vortex over the wing surface at low angle of attack. As alpha increases, this vortex widens, covering a large portion of the wing, disappearing at moderate angle of attack. Suction affects surface pressure distribution at low to moderate angle of attack, while its effect diminishes at a high angle of attack. It modifies the velocity profile shape near the surface.

1 Introduction

In designing a fighter aircraft, it is most important to increase its maneuverability at moderate to high angles of attack without deteriorating its stability and control criterion. Highly sweep-back wings have been used for these aircrafts mainly to prevent flow separation when operating at high angles of attack. However, depending on the wing sweep angle, the flow field over the wing surface separates at a certain angle of attack, degrading aerodynamic performance. Various concepts have been used to prevent or delay separation.

Boundary layer control remains one of the most promising avenues delaying for transition and separation, thus improving aircraft performance. A primary objective of the boundary layer control has always been that of allowing the flow over the wing surface to be diffused to the trailing edge without massive separation.

The second object being pursued very actively at present is delaying the boundary layer transition phenomenon hence forcing the flow to remain laminar instead of turbulent over the vehicle [1]. This process will cause substantial reduction in the skin friction drag of the immersed body.

There are three methods for stabilizing a boundary layer and delaying separation: 1) shaping the surface to provide long runs of favourable pressure gradient, 2) providing more stable boundary layer through suction, and 3) providing more stable boundary layer through surface cooling [2].

Boundary layer control as an aerodynamic art has been practiced through the 20th century. The state of the art as of 20 years ago has been subject of several studies [3]. The last 25 years have witnessed a fairly continuous effort at developing the technology for laminar flow aircrafts using surface suction. The difficulties of maintaining the aerodynamic surfaces with their numerous suction slots have triggered many thoughts and developments [3, 4].

In the experimental studies presented herein a suction system has been used to delay flow separation over the wing of a fighter type configuration operating at subsonic speeds and

at low to moderate angles of attack. The wing has a 40 degrees sweepback at the leading edge. Both spanwise surface pressure distribution and velocity profile at various angles of attack for suction on and off cases have been measured at two different Reynolds numbers. Some flow visualization tests including smoke visualization and tufts were carried out to investigate the flow patterns at various angles of attack. The results confirm presence of a relatively weak vortex on the wing at angles of attacks of about 6 degrees.

2 Experimental Apparatus

Figure 1 shows the model used for these investigations. It consists of an axisymmetric body with a conical nose and a flat plate cropped delta wing with a leading edge sweep angle of 40°. The model is similar to the HARV model used in various European wind tunnels for force and moment measurements [5-7]. However, to authors' knowledge, studies including velocity field, boundary layer and surface pressure measurements over this configuration have not been done yet. An extensive low speed experimental investigation including the aforementioned studies as well as canard and its position effects on the surface static pressure has been conducted at Sharif University of Technology, Department of Aerospace Engineering. The selected wing has a chamfered edge and is equipped with small holes for measuring surface pressure at various angles of attack.

Static pressure as well as total pressure has been measured using highly sensitive pressure transducers. Data for each transducer was collected via a multiplexer and transferred to the computer through a 16 bit analog to digital (A/D) board. The 16-bit A/D board was selected to increase the system accuracy. Various sampling rates were performed and finally the best one was selected. Tests were performed for clean model and model with two types of surface roughness using sand papers located at the wing leading edge.

All tests were conducted for suction on and off cases at various angles of attack. These experiments were carried out in the subsonic wind tunnel at the Sharif University of Technology, Department of Aerospace Engineering. The tunnel is of blow-down type with an approximately 45x45 *cm* test section, 100 *cm* in length. It operates at speeds ranging from 5 to 45 *m/s* with the diffuser installed [8] and uses 4 screens and a honeycomb in its settling chamber to break down the incoming free stream vortices. Figure 2 shows the test section with model installed in it. In figure 3 variations of the test section turbulence intensity with speed measured by a hot wire anemometer is shown. In this paper the flow field measurement data for clean model are presented.

3 Experimental results

Figures 4.a-g shows the flow field over a delta wing with leading edge sweep of 70°, two swept wings with sweeps of Λ=30° and Λ=45°, a cropped delta wing with Λ_{LE}=30° and the tuft visualization results of the present investigations. As can be seen, a pair of counter-rotating vortices primarily dominates the flow over a delta wing at moderate to high angle of attack. These vortices contain a large amount of energy and remain stable for a wide range of angles of attack. The surface oil-flow patterns shown over two swept wings, figures 4.b and c indicate the existence of a vortex sheet, an attachment line, and vortex burst phenomenon, figure 4.b. As the wing sweep angle increases, figure 4.c, Λ=45°, the vortex is seemed to align itself with the free stream, similar to that of delta wing, figure 4.a. The vortices formed over these wings, figures 4.b and c, are somehow similar to delta wing vortex but do not contain as much energy as the delta wing vortices do. This vortex is shed from the wing apex and moves towards the wing tip. From there it becomes parallel to free stream flow. The movement of these shed vortices towards the wing tip is probably due to the cross flow velocity component over the wing surface. Also shown in figure 4 is the low speed flow pattern over a cropped delta wing with leading edge sweep of Λ_{LE}=30°, visualized by oil strakes at two angles of attack, α=6°, and 12°, figures 4.d

and e. At low angle of attack, α=6°, the flow is characterized by completely attached flow with a weak tip vortex and a weak leading edge bubble, figure 4.d. The oil accumulation along the entire leading edge is an indication of the leading edge bubble, which is formed by the flow separation from the leading edge of the outer panel and reattaching on the surface again. However, for this angle of attack, α=6°, no separation is observed as shown by the straight attached lines. At 12° angle of attack, figure 4.e, the flow pattern is completely different. The wing tip vortex is still visible, but the attached flow region is less than that shown in figure 4.d. Instead there exists a large region of reversed flow and a large leading edge and wing tip separation regions. This phenomenon causes a large decrease of lift along with a change in the pitching moment variation. Shown in figure 4 is also the tuft flow visualization result of the present experiments. As can be seen, at low angle of attack, the tufts are moved toward the wing tip indicating the type of flow shown in figures 4.c and e. However, as the angle of attack increases, flow field study shows that the vortex covers a large portion of the wing and its shape is similar to that of delta wing vortices when they burst. The reason for the differences in the flow field seen between figures 4.e and f with those of figures 4.b-d is probably due to the differences in the shape of the wings, sweep angles, and the airfoil shape. The present wing has a flat plate airfoil with a chamfered leading edge. However, the characters of the flow over all 3 wings are similar.

Figures 5 and 6 show velocity contours over the wing surface at two different stations X/C=0.6 and X/C=0.8 and at angles of attack of 6, 12, and 18 degrees. From these figures, the formation of leading edge vortices and their expansion over the wing surface with increasing angle of attack is similar to those seen from figures 4.b-g. Comparison of figures 5.a and 6.a show that the leading edge vortex rises from the wing surface as the distance from the wing apex increases, typical of delta wing vortices. At angle of attack of 12 degrees, the vortex covers almost 2/3 of the wing's surface (figures 5.b, and 6.b), while at angle of attack of 18 degrees, the entire wing surface is covered by the vortical type flow (figures 5.c and 6.c).

Figures 7 and 8 show spanwise static pressure distribution over the wing surface at various angles of attack, α=2°-18°, and at two different stations, X/C=0.6 and 0.8. As seen from these figures, at low angles of attack, α=2° and α=6°, pressure distribution along the span decreases slightly from the wing root to the wing tip, indicating potential flow, similar to the oil data shown in figure 4.d. However, for higher angles of attack, α=10° and α=14°, a large portion of the wing surface is dominated by the low pressure, indicating the presence of the vortex. The surface covered by this vortex increases as the angle of attack increases from 10° to 18°. Also, from both figures, figures 7 and 8, note that as alpha increases the point of minimum pressure moves close to the wing root. This point, minimum pressure, is an indication of the vortex core, shown in figure 4.a known as primary vortex core. Surface pressure distribution for other velocity shows similar trend [12].

Figures 9 and 10 show the effect of suction on the spanwise pressure distribution for two angles of attack α=10° and α=18° and for two different stations, X/C=0.6 and 0.8. As seen from these figures, suction decreases surface pressure slightly. Its effect is more pronounced in the vicinity of the vortex core, while for the portion of the wing where pressure is constant, potential flow, suction has almost no effect as it should. Also, from both figures it can be noted that the effect of suction at higher angles of attack is more pronounced than at lower alpha. This is probably due to the fact that at low alpha the vortex is attached to the wing surface while by increasing the angle of attack, it lifts up from the surface before it breaks down. Hence, at high angle of attack when the suction is applied, it will decrease the distance between the vortex core and the wing surface.

Velocity profiles over the wing at five different stations for the angle of attack of 14 degrees and at two different stations, X/C=0.6 and X/C=0.8, are shown in figures 11.a and b.

These profiles were obtained using a pitot rake tube. The profiles at each station show the height of the vortices, their core, their strength, and finally their growth with increasing of *X/C*'s.

Effects of model angle of attack on the wing velocity profile at *X/C*=0.8 and at various spanwise locations are shown in figure 12. Note that due to restriction in the pitot rake tube movement and the diameter of its tubes, the closest distance from the wing surface where data could be acquired was about 2 *mm*, as shown by the symbols in figure 12. This figure clearly displays the type of flow over the wing surface, formation and expansion of vortices and their separation as well as their variation along the wing span. It can also be noticed that at low angles of attack, namely α=2°, the flow over the wing is almost potential, with a small classic boundary layer profile and a velocity less than the free stream velocity. At higher angle of attack, α=6°, the vortex begins to form and with increasing alpha, the magnitude of velocity increases too, indicating strength of the vortex. Also as the angle of attack increases, the vortex core moves upward, forming a secondary vortex beneath it (not shown in this figure). The velocity profiles at other stations show a similar trend and are not presented in this paper. Interested readers are referred to reference [12] for further details and findings.

Figures 13 and 14 show the effect of suction on the velocity profiles over the wing surface when set to α=6° and at different spanwise stations for two free stream velocities of 13 and 30 *m/s*. The suction rate for this investigation was constant, about 12 *lit/min*. For this suction rate, as seen in these figures, the velocity profiles in the vicinity of the surface have been influenced by the suction. Further from the wing surface no variation in the velocity profile due to the suction is observed. This is because in the region where the vortex exists, to have some effect on the vortex profile, the suction rate must be increased. But as stated, for these tests the suction rate was constant. Comparing figures 13 and 14, it is clear that the suction has more influence on a velocity profile with lower free stream velocity. As the angle of attack increases, the effect of suction with the current rate diminishes which is not shown in this paper. The effect of suction on the velocity profile at various angles of attack and different spanwise and chordwise stations are given in reference [12].

4 Conclusion

As a part of an ongoing research at the Department of Aerospace Engineering of Sharif University of Technology, velocity profile and surface static pressure were measured both with and without suction on the wing of a HARV model. Effect of surface roughness on the wing static pressure distribution was also studied. In this paper, results of flow field measurements for both suction on and off cases, were presented. The following results were obtained:

1. The flow field on the wing surface is similar to that of delta wings with low sweep angle with some differences.
2. At low angles of attack, the flow field over the wing surface is almost potential with a classical boundary layer.
3. The velocity profile over the wing surface at moderate angle of attack differs from that of straight or swept wing, indicating the existence of a vortex.
4. With increasing angle of attack the vortex widens, covering a large portion of the wing surface.
5. Suction has remarkable influence on the velocity profile when the model is set to low angles of attack. At high angle of attack and higher velocity the effect diminishes.

Further measurements are underway to better understand the flow field and the parameters that affect it over this type of wing planform.

References

[1] Hough GR (ed.). Viscous flow drag reduction. *Progress in Astronautics and Aeronautics*. Vol. 72, pp 185, 1979.

[2] Reshotko E. Drag reduction by cooling in hydrogen-filed aircraft. *Journal of Aircraft*, Vol. 16, pp 584-590, 1979.

[3] Gad-el-Hak M. Flow control: The future. *Journal of Aircraft*, Vol. 38, No.3, pp 402-419, 2002.

[4] Lachrnann GV. (ed.). *Boundary layer and flow control*. London. Program Press, 1961.

[5] Lang J. D. and Francis M. Unsteady aerodynamics and dynamics aircraft maneuverability. *AGARD-CP-38*, pp 29-1 to 29-19, 1985.

[6] Huenecke K. Low speed characteristics of a fighter-type configuration at high angles of attack and sideslip. *ICAS-82-5.8.1*, 1982.

[7] Hummel D and Oelker H. Low speed characteristics for the wing-canard configuration of the international vortex flow experiments. *Journal of Aircraft*, Vol. 31, No. 4, 1994.

[8] Soltani M. R and Davari, A. R. Experimental study of the flow field over a low aspect ratio wing. Journal of Esteghlal, Sep. 2001.

[9] Soltani, M. R. An experimental study of the relationship between forces and moments and vortex break down on a pitching delta wing. PhD. Thesis, University of Illinois at Urbana-Champaign, 1992.

[10] Poll, D. I. A. On the Generation and Subsequent development of spiral vortex flow over a swept back Wing. *AGARD-CP-342*, 1983.

[11] Liu, M. J., et-al. Flow patterns and aerodynamic characteristics of a wing-strake configuration. *Journal of Aircraft*, Vol. 17, No.5, 1980.

[12] Khadivi, T. Effects of surface roughness and flow suction on mean pressure distribution over the wing of a highly maneuverable aircraft. M.Sc Thesis, Department of Aerospace Engineering, Sharif University of Technology, 2001.

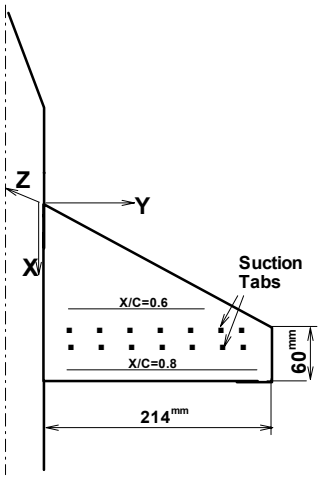

Figure 1. Schematic of the model

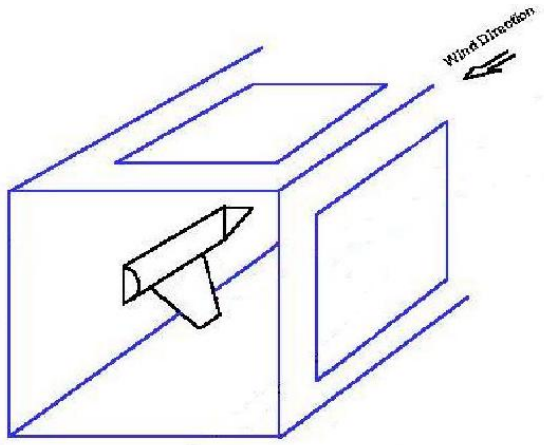

Figure 2. Test section and model

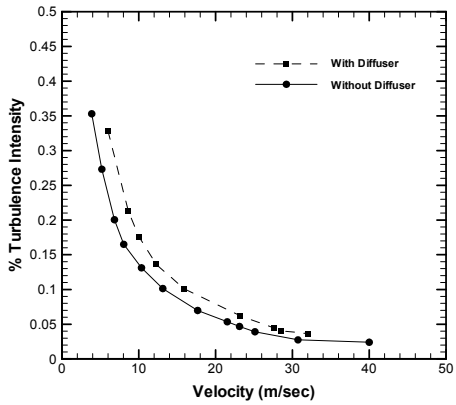

Figure 3. Variation of test section turbulence intensity with speed [8]

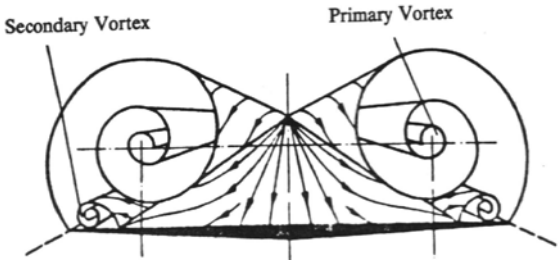

a) Delta wing, Λ=70° [9]

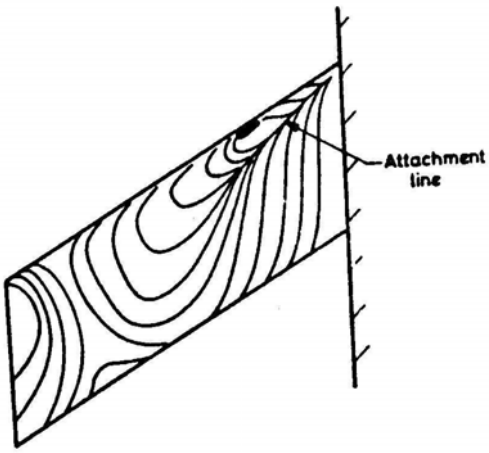

b) Swept wing, Λ=30°, α=10° [10]

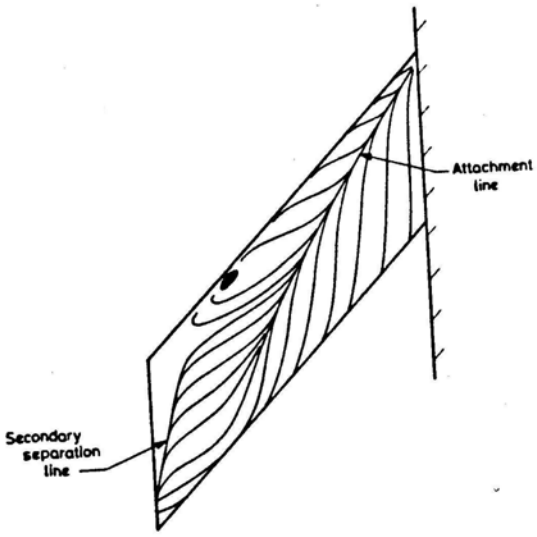

c) Swept wing, Λ=45°, α=11° [10]

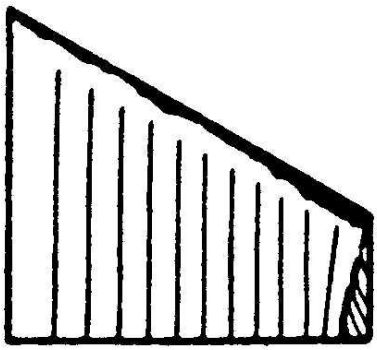

d) Cropped delta wing, Λ_{LE}=30°, α=6° [11]

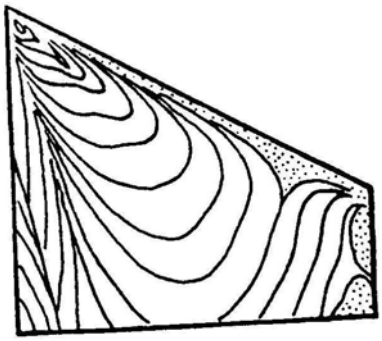

e) Cropped delta wing, Λ_{LE}=30°, α=12° [11]

f) The tuft visualization result, α=6° [12]

g) The tuft visualization result, α=10° [12]

Figure 4. Flow field over several wing planforms

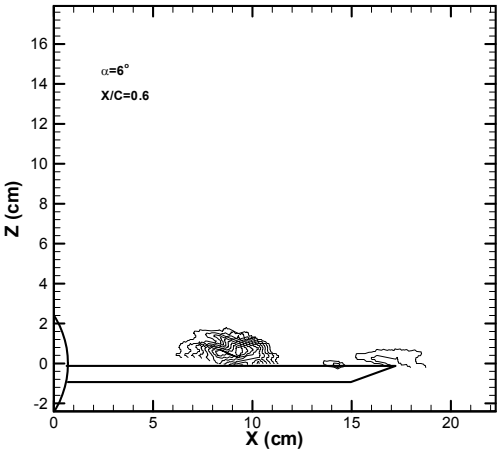

a) α=6°, X/C=0.6

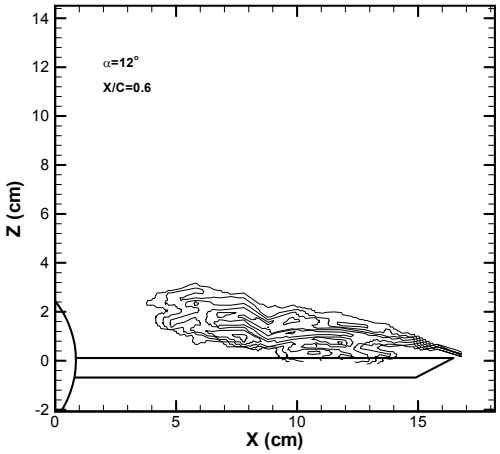

b) α=12°, X/C=0.6

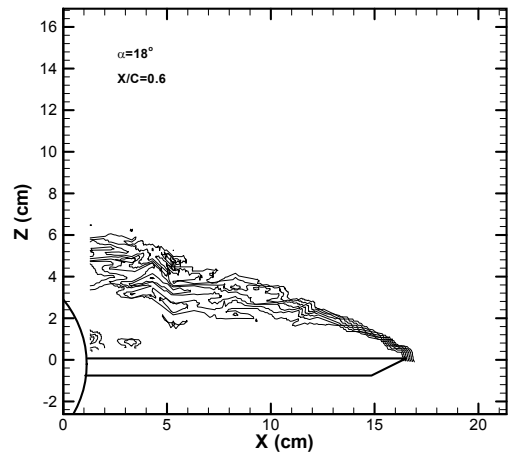

c) α=18°, X/C=0.6

Figure 5. Velocity Contour

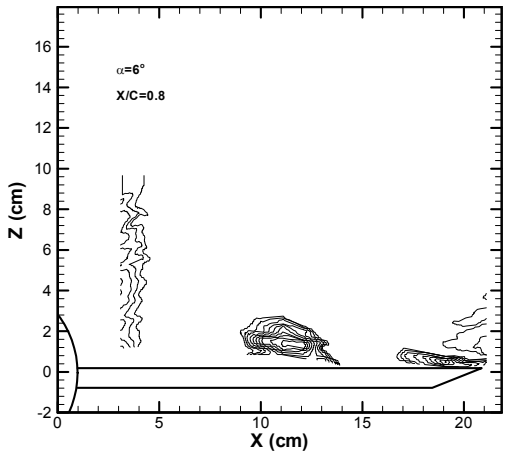

a) α=6°, X/C=0.8

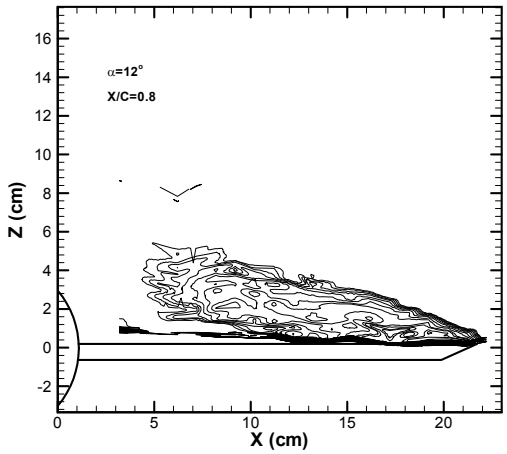

b) α=12°, X/C=0.8

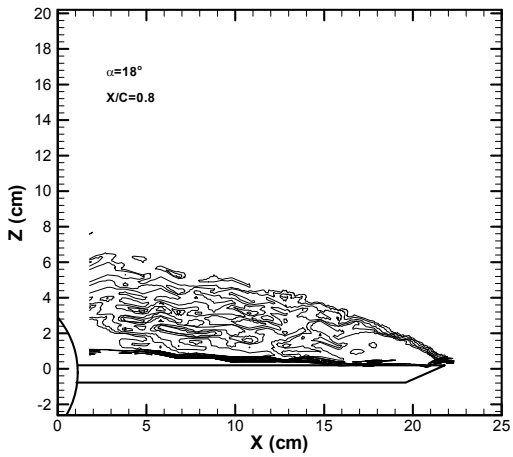

c) α=18°, X/C=0.8

Figure 6. Velocity Contour

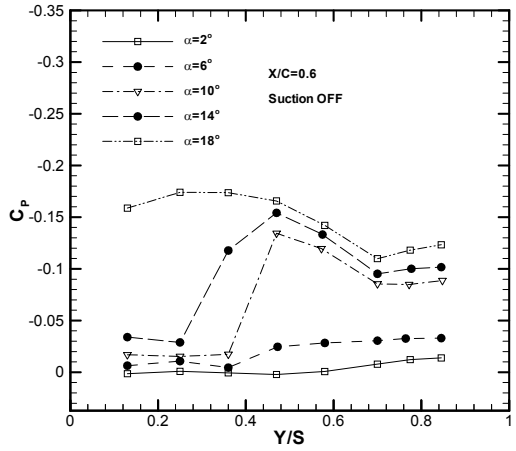

Figure 7. Spanwise pressure distribution, *X/C*=0.6

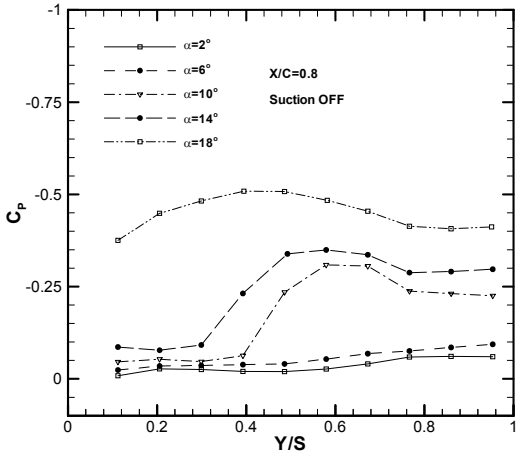

Figure 8. Spanwise pressure distribution, *X/C*=0.8

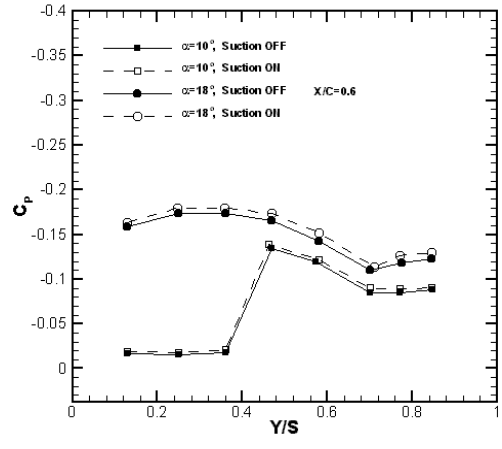

Figure 9. Effect of suction on the spanwise pressure distribution, *X/C*=0.6

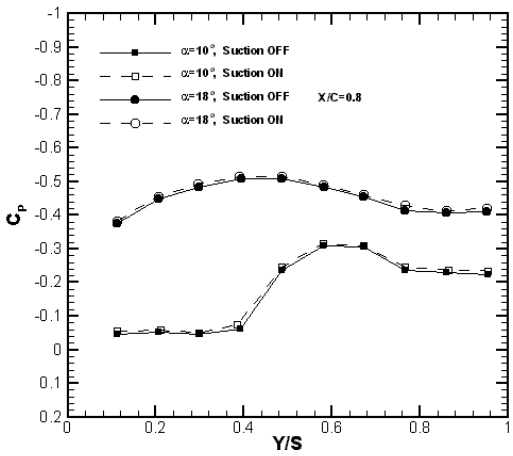

Figure 10. Effect of suction on the spanwise pressure distribution, *X/C*=0.8

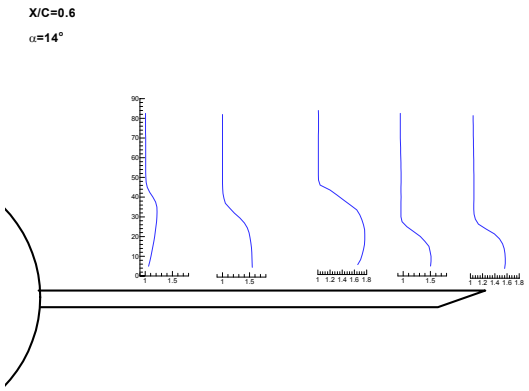

a) α=14°, *X/C*=0.6

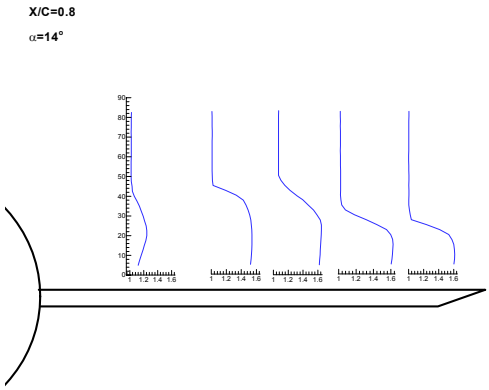

b) α=14°, *X/C*=0.8

Figure 11. Velocity profile over the wing surface

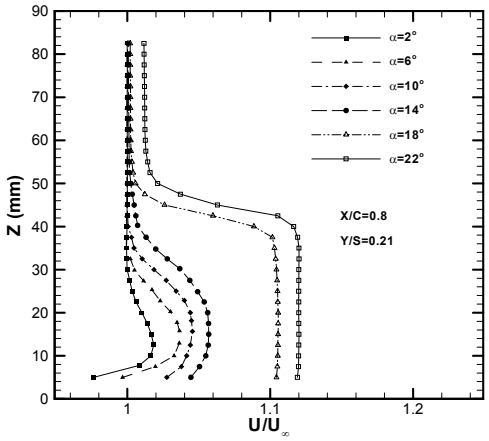

a) *Y/S*=0.21

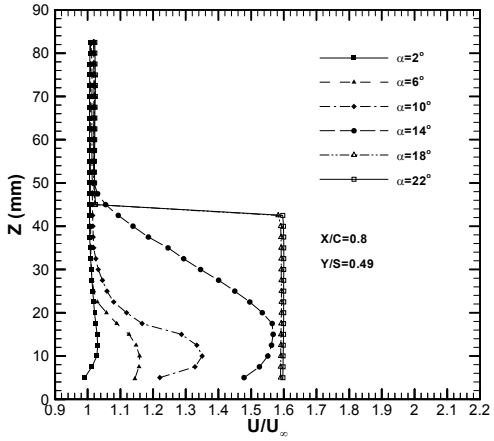

b) *Y/S*=0.49

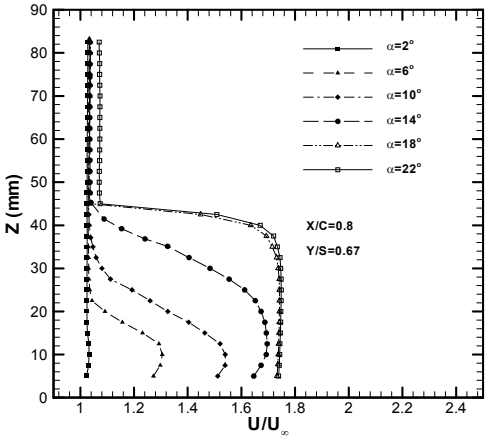

c) *Y/S*=0.67

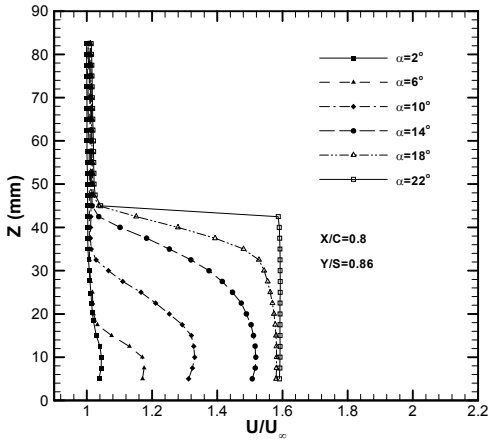

d) *Y/S*=0.86

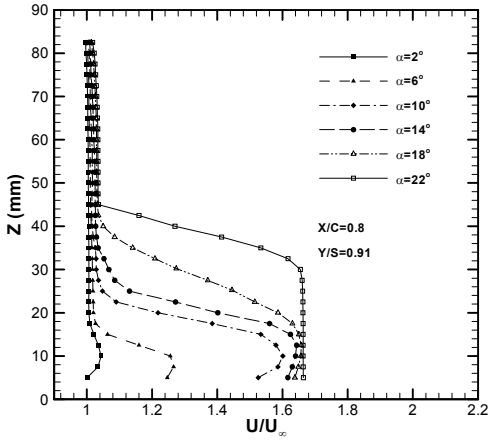

e) *Y/S*=0.91

Figure 12. Velocity profiles at *X/C*=0.8 & $U_\infty = 30\ m/s$

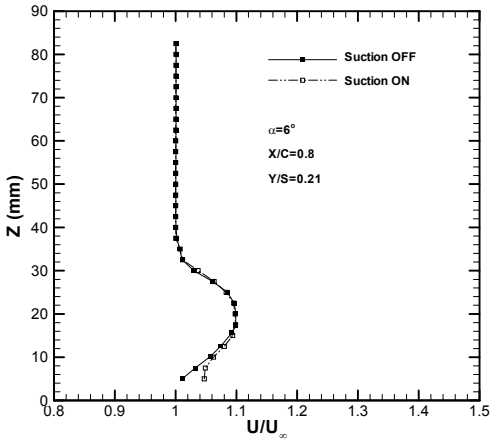

a) *Y/S*=0.21

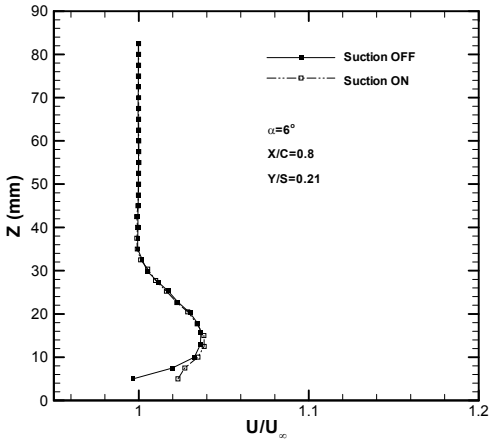

a) *Y/S*=0.21

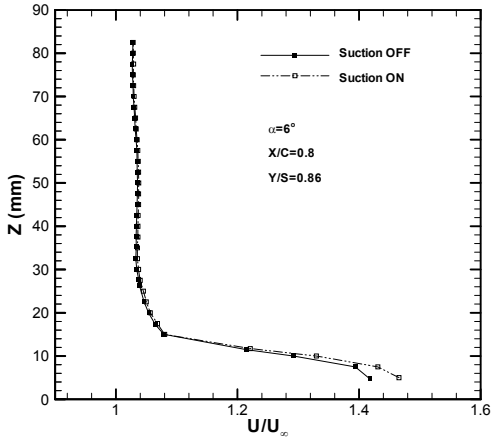

a) *Y/S*=0.86

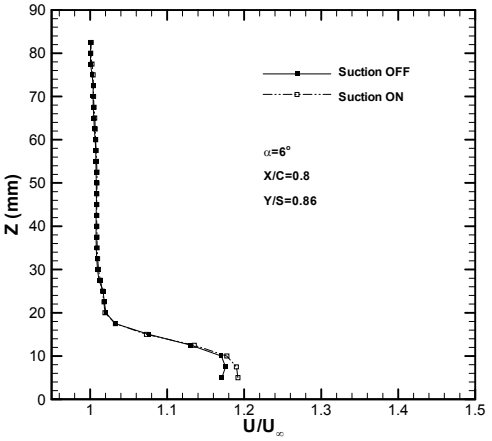

b) *Y/S*=0.86

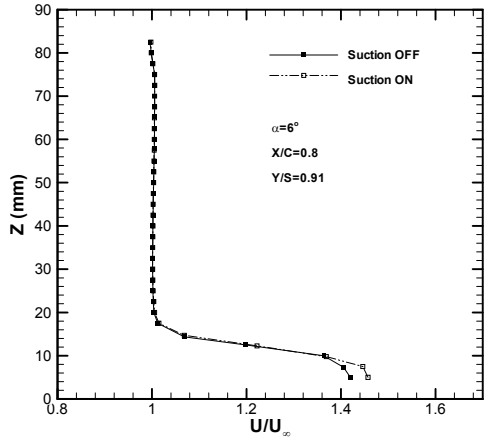

a) *Y/S*=0.91

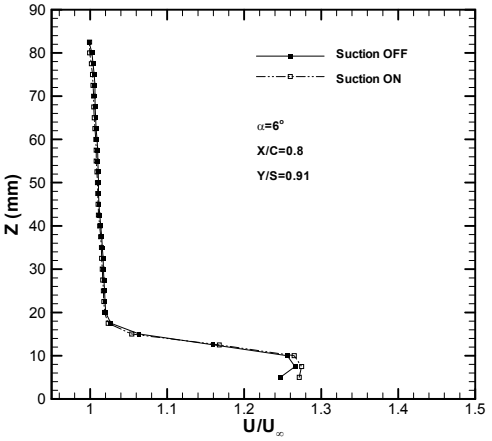

c) *Y/S*=0.91

Figure 13. Effect of suction on velocity Profiles, $U_\infty = 13\ m/s$

Figure 14. Effect of suction on velocity Profiles, $U_\infty = 30\ m/s$